Electrochemistry of 2,6-diaminopurine on multiwall carbon nanotube modified glassy carbon electrode

Ebru MAVİOĞLU AYAN, Şükriye ULUBAY KARABİBEROĞLU, Zekerya DURSUN*

Department of Chemistry, Faculty of Science, Ege University, 35100 Bornova, İzmir, Turkey

Abstract: The electrochemical oxidation of 2,6-diaminopurine (2,6-DAP) was studied in pH 7.4 phosphate buffer solution on multiwall carbon nanotube modified glassy carbon electrode (MWCNT/GCE) over a temperature range of 20 to 50 °C using cyclic voltammetry. 2,6-DAP oxidation on MWCNT/GCE showed a well-defined and irreversible oxidation peak at about 0.72 V vs. Ag/AgCl at pH 7.4. The oxidation potential of 2,6-DAP linearly varied with pH over the range of 3.0 to 10.0 with a slope of –0.0547 V/pH, implying that 2 protons were accompanied by 2 electrons transferred in the electrochemical reaction. The activation energy, Ea, of oxidation reaction was found to be 33.10 ± 1.88 kJ/mol. The differential pulse voltammetric determination of 2,6-DAP was also studied. The peak currents increased linearly with increasing of the 2,6-DAP concentration range from 0.4 μmol/L to 80 μmol/L. The linear regression equation appeared as $I_p/\mu A$ = –(1.66 ± 0.42) + (4.21 ± 0.11) [2,6-DAP]/μmol/L, R^2 = 0.9982, and the detection limit (S/N = 3) was 3×10^{-7} ± 0.015 mol/L (n =3). The electrocatalytic oxidation of 2,6-DAP on MWCNT/GCE showed that acid pretreated multiwall carbon nanotube can be used in new applications in electrochemical determinations of biologically important compounds.

Key words: Carbon nanotubes, 2,6-diaminopurine, activation energy, voltammetry

1. Introduction

Purine and pyrimidine derivatives are fundamental compounds in biological systems, playing an essential role in various biological processes such as energy transduction and cell signaling.[1−3] Substituted purines and pyrimidines constitute the backbone of DNA bases and RNA molecules. The clinical efficiency of several purine derivatives has been responsible for their use in human cancer therapy, virus infection, and vascular diseases. These, including 2,6-diaminopurine, 8-azoguanine, 6-mercaptopurine, thioguanine, 6-chloropurine, and other derivatives, are comparatively effective as anticancer agents.[4,5]

Determination of extracellular concentrations of purines is very important because changes in the concentrations can indicate several dysfunctions or diseases.[6] Many methods have been developed for the detection and quantification of purine bases in nucleic acids. Among them, the most commonly used are the spectroscopic methods,[7,8] chromatography,[9,10] and capillary electrophoresis,[11] although the voltammetric methods are practically suited for the analysis of these purines. In these methods, polythionine/gold nanoparticles/multiwall carbon nanotube modified glassy carbon electrode (GCE),[12] Nafion–ruthenium oxide pyrochlore modified GCE,[13]

---

*Correspondence: zekerya.dursun@ege.edu.tr

carbon nanotube modified GCE,[14−18] mercury electrode,[19,20] and so on were used for determination of purines and purine derivatives.

2,6-Diaminopurine (2,6-DAP) is obtained from adenine, substituting an additional amino group into position 2. It is one of a large class of compounds, analogs of natural purines, that show pharmacological properties as antimetabolites of nucleic acid metabolism. 2,6-DAP has been shown to act as a growth inhibitor of bacteria and mammalian cells.[21−24] Determination of 2,6-DAP was studied by differential pulse voltammetry at graphite electrodes in pH 7 phosphate buffer solution and the linear range for 2,6-DAP was found as ranging from 1.0×10^{-6} to 5.0×10^{-4} mol/L.[21] Electrochemical oxidation of aminopurines and their complexes with Cu(I) was investigated on a pencil graphite electrode by voltammetric technique. The determination of aminopurines was based on the formation of a complex between cuprous ions and aminopurine molecules, its adsorption on the electrode surface, and dissolution by oxidative stripping.[25]

Because carbon nanotube (CNT) has outstanding advantages such as high conductivity, high chemical stability, and extremely high mechanical strength and modulus, it is widely used in many fields, including in nanoelectronic devices, electron field emission sources, and potential hydrogen storage materials. In addition, CNTs are used as electrode materials in the electroanalytical field for their good capability of electron transfer.[26−28] It has been reported that CNT modified electrodes were successfully applied to study and determine many biological and organic molecules, such as dopamine,[30−32] ascorbic acid,[33,34] uric acid,[34,35] cytochrome C[36] NADH,[37] amino acids,[38] hydrazine,[39] nitrite,[40] adenine and guanine,[14,41,42] and DNA.[43]

A search of the literature clearly reveals that there are no reports for activation energy and voltammetric determination of 2,6-diaminopurine on multiwall carbon nanotube modified glassy carbon electrode (MWCNT/GCE). In this paper, for the first time, the MWCNT/GCE was used to obtain the activation energy depending on temperature by measuring the peak current and peak potential of 2,6-DAP on cyclic voltammograms. The differential pulse voltammetric technique was also used for sensitive determination of 2,6-DAP.

2. Experimental

2.1. Chemicals

MWCNTs were purchased from Aldrich Chem. with a diameter of 110–170 nm, a length of 5–9 μm, and purity of 90%, and they were purified with concentrated HNO_3. 2,6-DAP was supplied by Aldrich Chem. All other reagents were of analytical grade and used without any further purification. The buffer solutions were prepared from acetic acid/sodium acetate (0.1 mol/L), sodium dihydrogenphosphate/disodium monohydrogen phosphate, and boric acid/sodium metaborate in the pH range of 3.0–10.0. Stock solution of 2,6-DAP was prepared daily with ultrapure water (Millipore Milli Q System, 18.2 Ω). All electrochemical measurements were obtained under pure N_2 atmosphere.

2.2. Apparatus

Voltammetric measurements were carried out using a Bas 100B electrochemical analyzer and IviumStat & IviumStat.XR electrochemical interface and impedance analyzer with a 3-electrode system consisting of a working electrode (bare GCE and MWCNT-GCE), a platinum wire counter electrode, and an Ag/AgCl (sat. KCl) reference electrode. Cyclic voltammetry (CV) and differential pulse (dp) mode were used throughout the electroanalytical studies. The pH measurements were made with a WTW handheld 330i ion analyzer pH meter. A Philips XL-30S SEM was used for the characterization of carbon nanotubes on the electrode surfaces.

The CV curves were obtained under nitrogen flow in the experiments of variable temperature. Temperatures were kept constant by water circulation through a double wall cell, which was connected to a Polyscience 901 Refrigerated Circulator.

2.3. Pretreatment of multiwall carbon nanotube and preparation of modified electrodes

The MWCNT, as received, was pretreated with concentrated HNO_3 for purification and activation as follows: 0.1 g of MWCNT was boiled in approximately 4 mL of concentrated HNO_3 for 30 min and then washed many times with ultrapure water. The acid-treated MWCNT was dispersed in DMF to get a black suspension by ultrasonic bath. Before modification, GCE was activated by polishing with a different grade of Al_2O_3 slurry (0.05–3.0 μmol/L) on a synthetic cloth, then rinsing with pure water and ultrasonication for 3 min in an ultrapure water and ethanol mixture. A 10-μL MWCNT suspension was injected on the preconditioned bare GCE surface and then the solvent (DMF) of the suspension on the GCE surface was evaporated at 55 °C at least 2 h to fabricate the MWCNT/GCE.

3. Results and discussion

3.1. Scanning electron microscopy and electrochemical impedance spectroscopy characterizations of MWCNT/GCE

The surface morphology of MWCNT modified GCE was studied by recording SEM images (Figure 1A). The image clearly indicates the deposition of MWCNT at the electrode surface. Figure 1B illustrates the results of electrochemical impedance spectroscopy (EIS) on bare GCE and MWCNT/GCE in the presence of 10 mmol/L $Fe(CN)_6^{3-/4-}$ + 0.1 mol/L KCl solution. At the bare GCE, a semicircle of about 1334 Ω in diameter with an almost straight tail line can be seen. However, the diameter of the high frequency semicircle was noticeably reduced to 990 Ω (found by extrapolation from Figure 1B) by the surface modification of the MWCNT, suggesting that a significant acceleration of the redox reaction $Fe(CN)_6^{3-/4-}$ occurred on the MWCNT surface. In Figure 1B, the slope of the curve is almost equal to 1, indicating that a mass controlled process takes place on the MWCNT/GCE surface.

3.2. Cyclic voltammetry characteristics of 2,6-diaminopurine on the MWCNT/GCE

The voltammetric behavior of 1.0×10^{-5} mol/L 2,6-DAP at the bare GCE (in Figure 2 inset) and MWCNT-GCE (curve b) are shown in Figure 2. A small broad oxidation peak for 2,6-DAP was observed at 0.78 V vs. Ag/AgCl, at bare GCE in pH 7.4 PBS. In the case of MWCNT/GCE, the main anodic peak (A_1) at 0.70 V vs. Ag/AgCl was related to the oxidation of 2,6-DAP. No cathodic peak was observed on the reverse scan, which displayed that 2,6-DAP oxidation was an electrochemically irreversible process at both bare and modified electrodes. On scanning in the negative direction, 2 peaks were displayed due to reduction of the oxidation product (C_1) and adsorption process (C_2). The peak current signal increased significantly with its peak potential shifting negatively for about 0.08 V vs. Ag/AgCl. A high electrocatalytic activity was observed at MWCNT/GCE towards the oxidation of 2,6-DAP at pH 7.4 PBS by means of significant peak current increase and peak potential shift.
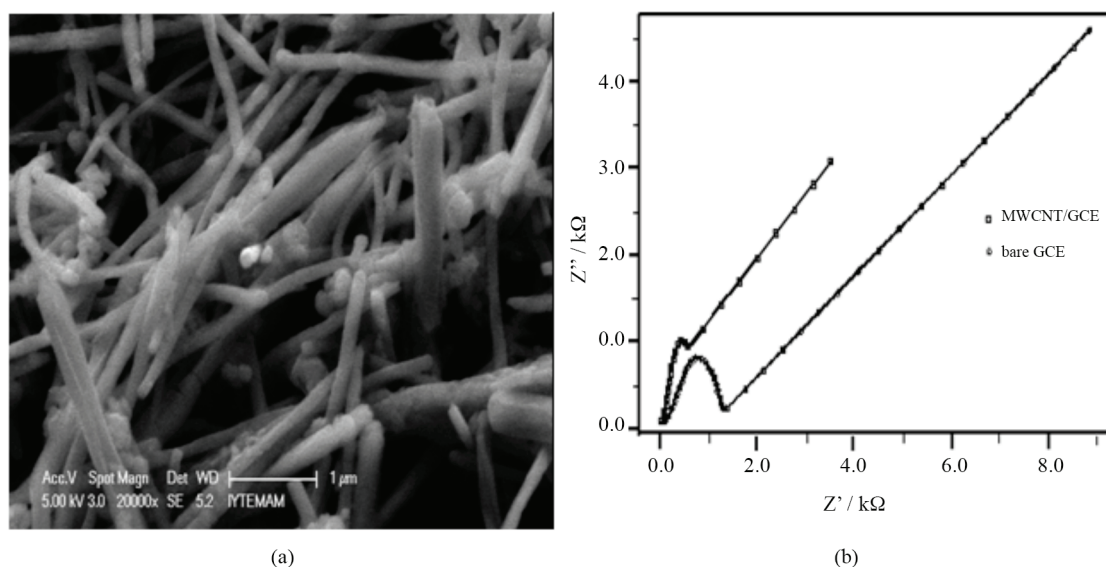
(a)

(b)

Figure 1. A) SEM images of MWCNT/GCE and B) electrochemical impedance curves of bare GCE ($\bigcirc$) and MWCNT/GCE ($\square$[U+FFFF])
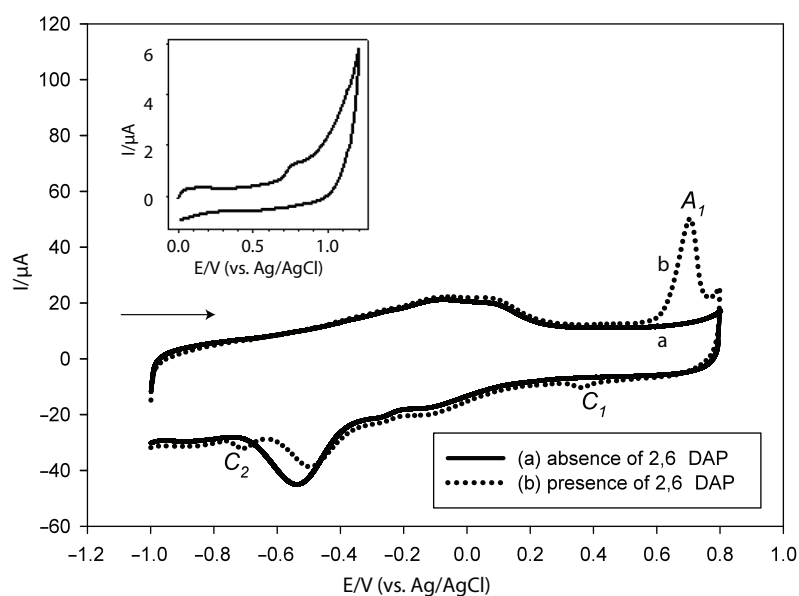

Figure 2. Cyclic voltammograms of 1.0×10^{-5} mol/L 2,6-diaminopurine oxidation at the bare GCE (inset) with absence (a) and presence (b) on MWCNT/GCE in pH 7.4 PBS. Scan rate: 0.05 V/s.

Successive cyclic voltammograms were recorded in a solution of 1.0×10^{-5} mol/L 2,6-DAP for pH 7.4 PBS at the MWCNT/GCE in the case of the narrow potential range from –0.25 V to 0.80 V (Figure 3A). The oxidation of 2,6-DAP, peak A_1, appears at 0.70 V. In the second CV scan, new 2 oxidation peaks, A_2 and A_3, were observed at 0.38 V and 0.50 V vs. Ag/AgCl, and their currents had almost no change with the increasing of the CV scan number. In the reverse potential scan, cathodic peak C_1 is observed at 0.35 V vs. Ag/AgCl, but the peak current is smaller than the A_1 current, suggesting that the oxidation product of

2,6-DAP is very unstable and undergoes hydrolysis on the electrode surface. According to cyclic voltammetric results, a 2-step electrode process can be suggested for 2,6-diaminopurine's possible oxidation mechanism at the modified electrode surface. In the first step, the oxidation process of 2,6-diaminopurine can be explained by transfer of 2 electrons to produce 2,6-diamino-8-hydroxypurine (II in Figure 4), and in the second step, the product of the first step can be oxidized after 2-electron transfer for producing the corresponding unstable diimine intermediates, given as III in Figure 4. In the end of the electrode process, the final-forming oxidation products were hydrolyzed in water to the ultimate compounds, such as parabonic acid, oxaluric acid, urea, ammonia, allontoin, and guanidine.[1,23,44]
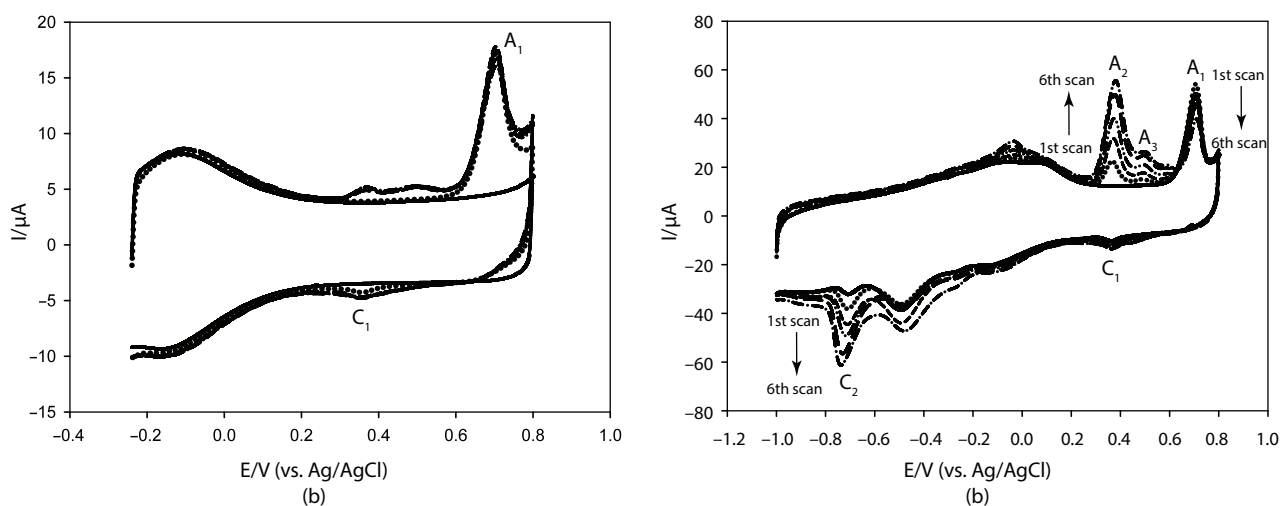

Figure 3. Cyclic voltammograms of 1.0×10^{-5} mol/L 2,6-diaminopurine oxidation at MWCNT/GCE consecutively recorded for A) narrow potential and B) large potential in pH 7.4 PBS. Scan rate: 0.05 V/s.
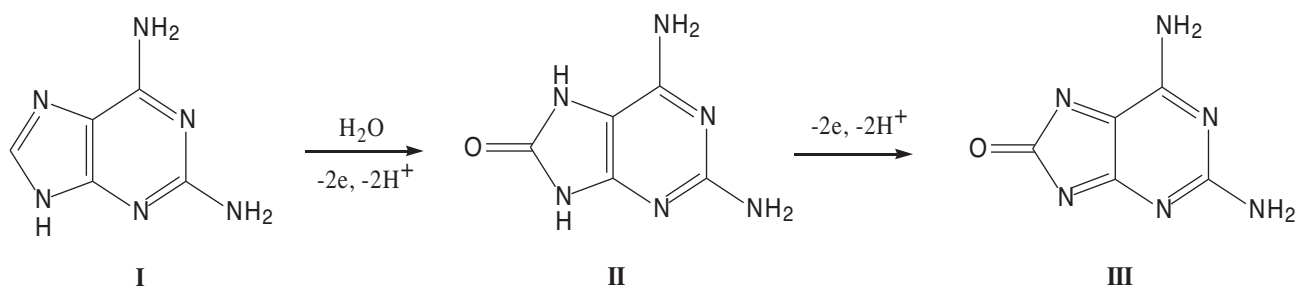

Figure 4. Proposed reaction mechanism for the electrochemical oxidation of 2,6-diaminopurine.

When the CVs were recorded in the large potential range from –1.00 V to 0.80 V (Figure 3B), only an oxidation peak appeared at 0.70 V vs. Ag/AgCl due to the oxidation of 2,6-DAP. After the first current potential CV scan, 2 new oxidation peaks, A_2 and A_3, were observed at 0.38 V and 0.50 V, and their currents increased with the increasing of the CV scan number. These peaks correspond to the oxidation of the product of oxidation of 2,6-DAP, 2,6-diamino-8-hydroxypurine, which is strongly adsorbed on the electrode surface. At the same time, the oxidation current of 2,6-DAP decreases gradually with the number of potential scans due to the decrease in the available electrode surface because of the adsorption of 2,6-diamino-8-hydroxypurine. In the

reverse cathodic potential scan, a second reduction peak, C_2, was observed at –0.73 V, and its height increased with the increasing of the CV scan number. The larger potential CV scan showed that the increasing of the C_2 peak height is strongly affected by A_2 peak height and its peak current directly correlated with the C_2 peak current increasing.

At the end of consecutive CV scans, the electrode was washed with deionized water and transferred to the supporting electrolyte. The oxidation peak of 2,6-DAP was observed in the supporting electrolyte, which did not contain 2,6-DAP. This result shows the adsorption of 2,6-diamino-8-hydroxypurine at the MWCNT/GCE.

According to the CV results in Figures 3A and 3B, the narrow potential range clearly showed a stable oxidation peak current at 0.70 V vs. Ag/AgCl for recording of repetitive CV scan. This is important for the study of the quantitative determination of 2,6-DAP with differential pulse voltammetry at MWCNT/GCE.

The effect of pH on the electrochemical oxidation of 2,6-DAP was studied over a wide pH range between 3.0 and 10.0 using CV. The cyclic voltammograms were all recorded for 1.0×10^{-5} mol/L 2,6-DAP at MWCNT/GCE. The peak potential was shifted to more negative values with increasing pH (Figure 5). Although a higher oxidation peak current was obtained at pH 6.0, pH 7.4 was chosen as the supporting electrolyte for biological pH in future voltammetric studies of 2,6-DAP. The potential is dependent linearly on pH over the whole range as follows:

$$E_p/V = (1.1082 \pm 0.0117) - (0.0547 \pm 0.0017)pH \tag{1}$$

The variation of Ep with pH could provide valuable information on the 2,6-DAP oxidation process. The peak potential was observed to decrease linearly versus increasing pH with a slope of 0.054 ± 0.0017 V/pH, which suggests that the same number of protons and electrons were involved in the oxidation process of 2,6-DAP.
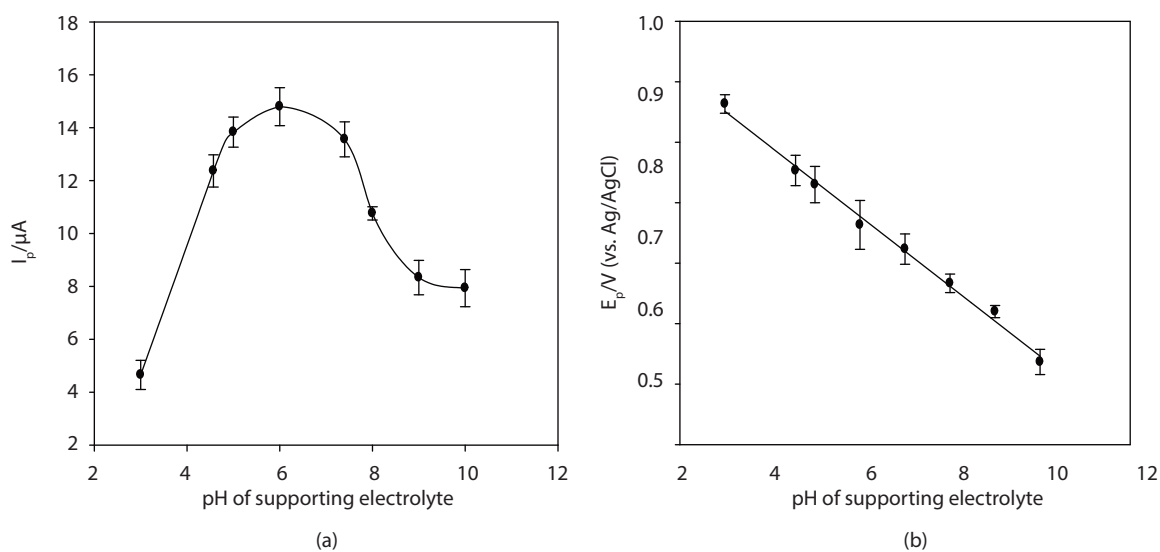

Figure 5. Effect of pH on the oxidation on A) I_p and B) E_p of 1.0×10^{-5} mol/L 2,6-DAP at MWCNT/GCE (E_p/V = (1.1082 ± 0.0117) – (0.0547 ± 0.0017) pH).

The scan rate effect on peak current and peak potential of 1.0×10^{-5} mol/L 2,6-DAP was studied over the range of 50–225 mV/s at MWCNT/GCE in 0.1 M PBS (pH 7.4) by cyclic voltammetry. The peak current increased linearly and followed the relationship of

$I_p/\mu A = (0.382 \pm 0.103) + (0.9386 \pm 0.0207) \, v^{1/2}/(mV/s)^{1/2}$ ($R^2 = 0.9961$) depending on the square root of the scan rate, which suggested diffusion control on the MWCNT/GCE surface electrode process, as shown in Figure 6A. The peak potential also shifted linearly with the square root of the scan rate and the curve equation was:

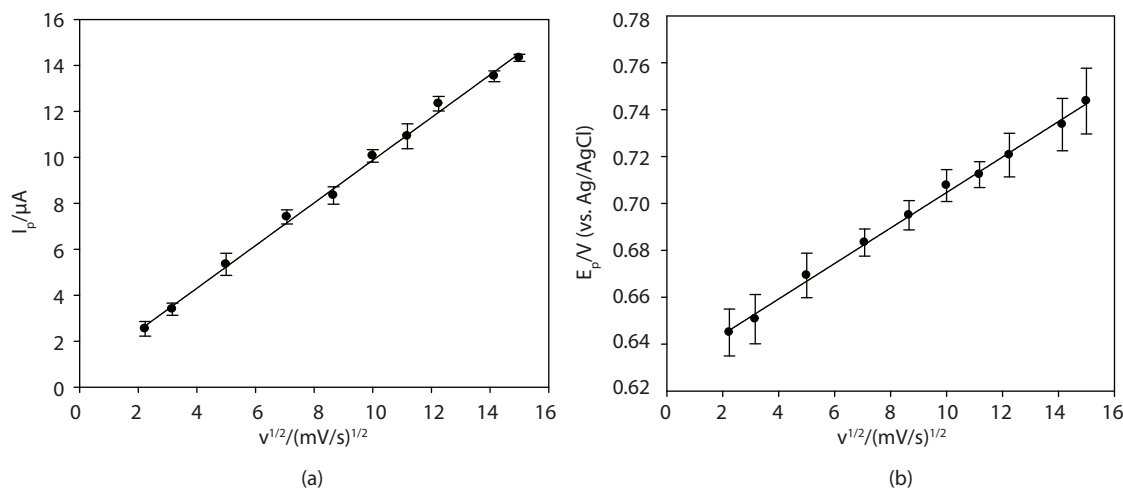$E_p/V = (0.6300 \pm 0.0021) + (0.0064 \pm 0.0002) \, v^{1/2}/(mV/s)^{1/2}$ ($R^2 = 0.9961$).

(a) (b)

Figure 6. Variation of 1.0×10^{-5} mol/L 2,6-DAP oxidation A) peak current ($Ip/\mu A = (0.382 \, (0.103) + (0.9386 \, (0.0207)v^{1/2}/(mV/s)^{1/2})$ and B) peak potential versus the square root of the scan rate (50–225 mV/s), $Ep/V = (0.6300 \, (0.0021) + (0.0064 \, (0.0002) \, v^{1/2}/(mV/s)^{1/2}$.

Those data also showed that an irreversible electrode reaction takes place on the MWCNT/GCE surface (Figure 6B).

3.3. Calculation of the activation energy of 2,6-DAP on the MWCNT/GCE depending on temperature

The effect of temperature on electrochemical oxidation of 2,6-DAP was studied for 1.0×10^{-5} mol/L 2,6-DAP in the temperature range between 21 and 49 °C. The peak current was increased by increasing the temperature while the peak potential shifted to negative values (Figure 7A). This indicates that the temperature increase causes the oxidation procedure to take place more easily on the MWCNT/GCE surface, due to the decrease in the activation energy.

The activation energy, Ea, can be calculated as outlined by Da Silva et al., where the rate of electrode processes can be expressed in terms of peak current (I_p) of the energy of the reactant.[45]

$$I_p = I_p^{\circ} \exp(-Ea/RT), \qquad (2)$$

where Ip° is a constant, Ea is the activation energy, R is the gas constant, and T is Kelvin temperature. Da Silva et al. demonstrated that activation energy is a function of the overpotential (η), which is related to α_T by the following the equation:[46]

$$E_a^{\eta} = Ea - \alpha_T F\eta, \qquad (3)$$

where α_T is the transfer coefficient at constant temperature and F is the Faraday constant.
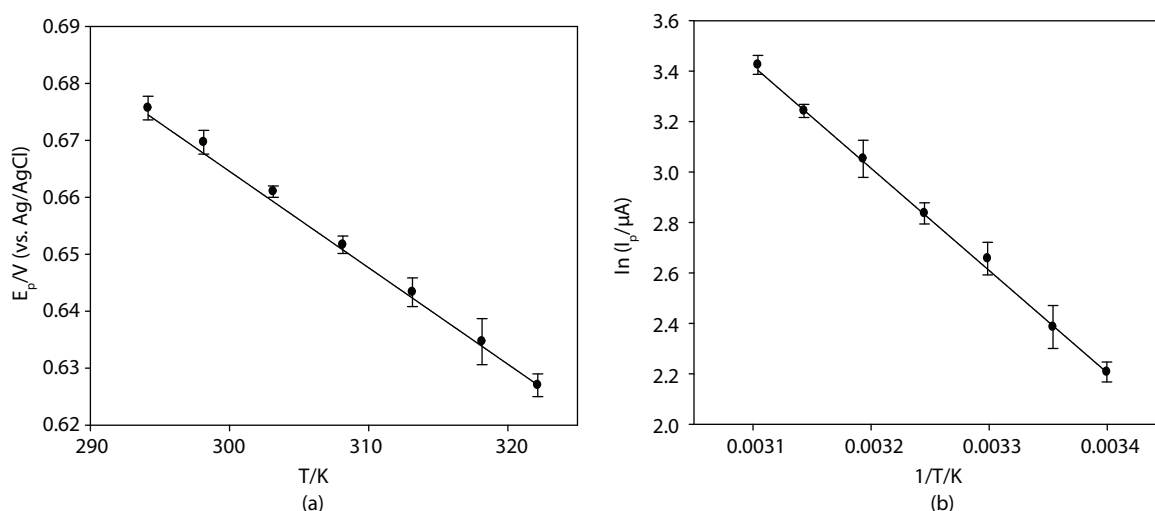
Figure 7. A) Temperature dependence of the oxidation potentials of 2,6-DAP in pH 7.4 PBS and B) Arrhenius plot for 2,6-DAP oxidation at 0.72 V.

Ea can be calculated from $\ln I_p / \mu A = f(1/T)$ (Arrhenius plot) by using the following relation:

$$\left(\frac{d \ln I_p}{dT^{-1}} \right) = \left(-\frac{E_a^\eta}{R} \right) \tag{4}$$

The slope of the plot in Figure 7B is –Ea/R with a value of –3981.6 $\pm$ 227.1. Ea was found to be 33.10 $\pm$ 1.88 kJ/mol. The activation energy of 2,6-DAP oxidation on bare GCE was also determined as 45.00 $\pm$ 2.01 kJ/mol, which was higher than that on the MWCNT/GCE. It was shown that the oxidation reaction of 2,6-DAP took place more easily compared to that on bare GCE.

3.4. Differential pulse voltammetric determination of 2,6-DAP

Differential pulse voltammetry (DPV) was used for the quantitative determination of 2,6-DAP. The peak current of DPV was linearly proportional to the concentration of 2,6-DAP. The DPV and calibration curves for oxidation of 2,6-DAP in pH 7.4 PBS at MWCNT/GCE are shown in Figures 8 and 9, respectively. The peak currents increased linearly with increasing 2,6-DAP in the concentration range from 0.4 μmol/L to 80 μ mol/L. The linear regression equation is $I_p / \mu A = -(1.66 \pm 0.42) + (4.21 \pm 0.11)$ [2,6-DAP]$/\mu$mol/L with $R^2 = 0.9982$, and the detection limit (S/N = 3) is $3 \times 10^{-7} \pm 0.015$ mol/L (n = 3) (Figure 9).

3.5. Stability of the MWCNT/GCE

The long-term storage stability of the MWCNT/GCE was studied by keeping the electrode in phosphate buffer solution (pH 7.4) at room temperature. The performance of MWCNT/GCE for the detection of 1.0×10^{-5} mol/L 2,6-DAP was tested in PBS of pH 7.4 for 1 week. Over the first 2 days, the oxidation of the 2,6-DAP signal decreased by 1.81%, and the oxidation current response maintained 92% of the original peak current value after 1 week. Therefore, the electrode could be used for almost 1 week without any significant error.
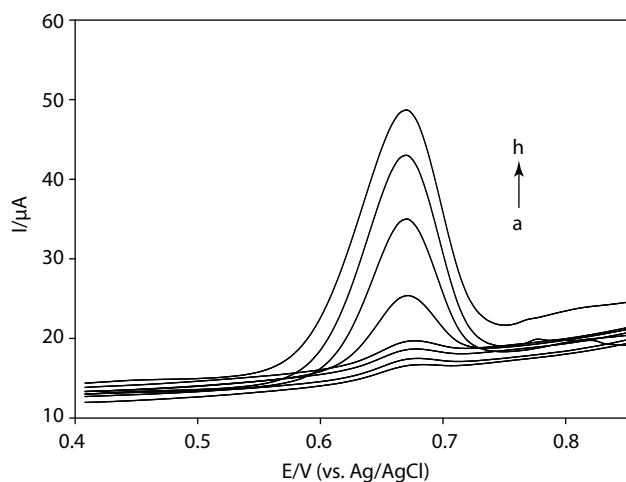
Figure 8. DPVs at MWCNT/GCE in 0.1 M pH 7.40 PBS; 2,6-DAP concentrations (a–h): 4.0×10^{-7} to 8.0×10^{-6} mol/L.
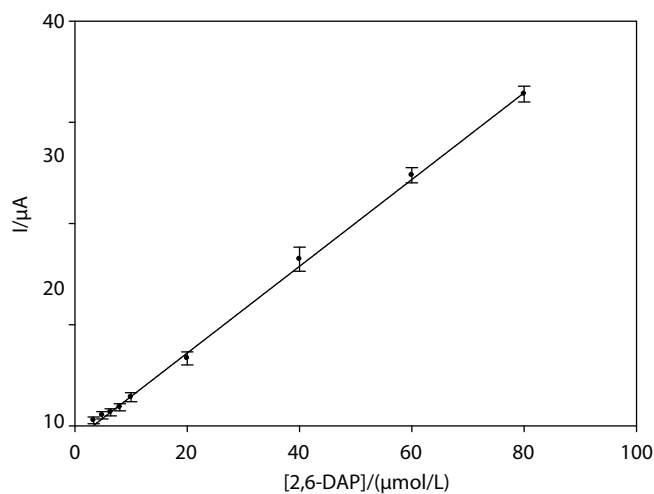
Figure 9. Calibration curve for 2,6-DAP concentrations from 0.4 μmol/L to 80 μmol/L. (I_p / μA $= -(1.66 \pm 0.42) + (4.21 \pm 0.11)$ [2,6-DAP]/μmol/L).

4. Conclusion

The electrochemical behavior of 2,6-DAP was studied by the electroanalytical method at a glassy carbon electrode modified with MWCNTs. A well-defined irreversible peak was obtained for oxidation of 2,6-DAP. The oxidation of 2,6-DAP at the MWCNT/GCE is a diffusion-controlled process involving 2 protons and 2 electrons. The activation energy also was determined by using temperature dependence of peak current and peak potential. The differential pulse voltammetric determination of 2,6-DAP was also studied. The peak currents increased linearly with increasing 2,6-DAP in the range from 0.4 μmol/L to 80 μmol/L. The linear regression equation was found as I_p / μA $= -(1.66 \pm 0.42) + (4.21 \pm 0.11)$ [2,6-DAP]/μmol/L, $R^2 = 0.9982$, and the detection limit (S/N = 3) was $3.0 \times 10^{-7} \pm 0.015$ mol/L (n = 3).

Acknowledgments

References

1. Diculescu, V. C.; Piedade, J. A. P.; Maria, A.; Brett, O. *Bioelectrochem.* **2007**, *70*, 141–146.

2. Goyal, R. N.; Gupta, V. K.; Oyama, M.; Bachheti, N. *Talanta* **2007**, *71*, 1110–1117.

3. Simoni, R. E.; Gomes, L. N. L. F.; Scalco, F. B.; Oliveira, C. P. H.; Neto, F. R. A.; Oliveria, M. L. C. *J. Inherit. Metab. Dis.* **2007**, *30*, 295–309.

4. Nayan, R.; Dey, A. K. *Z. Naturforsch.* **1972**, *27*, 688–690.

5. Yan, X.; Li, H.; Xu, Z.; Li, W. *Bioelectrochem.* **2009**, *74*, 310–314.

6. Xie, X.; Yang, K.; Sun, D. *Colloid. Surface. B* **2008**, *67*, 261–264.

7. Amri, C. E.; Maurel, M. C.; Baronc, M. H. *Spectrochim. Acta Part A* **2005**, *61*, 2049–2056.

8. Amri, C. E.; Baronc, M. H.; Maurel M. C. *Spectrochim. Acta Part A* **2003**, *59*, 2645–2654.

9. Gill, B. D.; Indyk, H. E. *Int. Dairy J.* **2007**, *17*, 596–605.

10. Ganzera, M.; Vrabl, P.; Worle, E.; Burgstaller, W.; Stuppner, H. *Anal. Biochem.* **2006**, *359*, 132–140.

11. Yeh, C. F.; Jiang, S. J. *Analyst* **2002**, *127*, 1324–1327.

12. Liu, H.; Wang, G.; Chen, D.; Zhang, W.; Li, C.; Fang, B. *Actuat. B Chem.* **2008**, *128*, 414–421.

13. Zen, J. M.; Chang, M. R.; Ilangovan, G. *Analyst* **1999**, *124*, 679–684.

14. Zhang, R.; Wang X.; Chen, C. *Electroanal.* **2007**, *19*, 1623–1627.

15. Lü, S. *Microchem. J.* **2004**, *77*, 37–42.

16. Abdullin, T. I.; Nikitina, I. I.; Bondar, O. V. *Russ. J. Electrochem.* **2008**, *44*, 1444–1448.

17. Wang, J.; Kawde, A. N.; Musameh, M. *Analyst* **2003**, *128*, 912–916.

18. Lu, B. Y.; Li, H.; Deng, H.; Xu, Z.; Li, W. S.; Chen, H. Y. *J. Electroanal. Chem.* **2008**, *621*, 97–102.

19. Jelen, F.; Kourilova, A.; Pecinka, P.; Palecek, E. *Bioelectrochem.* **2004**, *63*, 249–252.

20. Trnkova, L.; Friml, J.; Dracka, O. *Bioelectrochem.* **2001**, *54*, 131–136.

21. Szurley, E.; Toth, A. B. *Anal. Chim. Acta* **1983**, *154*, 323–327.

22. Astwood, D.; Lippincott, T.; Deysher, M.; D'Amico, C.; Szurley, E.; Toth, A. B. *J. Electroanal. Chem.* **1983**, *159*, 295–312.

23. Yao, T.; Musha, S. *Bull. Chem. Soc. Japan* **1979**, *52*, 2307–2311.

24. Mavioğlu, E. *Determination of the Thermodynamic Stability Constants and Thermodynamic Parameters of Metal Complexes of Some Purines*, MSc Thesis, Ege University, 2001.

25. Aladag, N.; Trnkova, L.; Kourilova, A.; Ozsoz, M.; Jelen, F. *Electroanal.* **2010**, *22*, 1675–1681.

26. Agüi, L.; Sedeno, P. Y.; Pingarron, J. M. *Anal. Chim. Acta* **2008**, *622*, 11–47.

27. Liu, G.; Riechers, S. L.; Mellen, M. C.; Lin, Y. *Electrochem. Comm.* **2005**, *7*, 1163–1169.

28. Wang, Y. R.; Hu, P.; Liang, Q. L.; Luo, G. A.; Wang, Y. M. *Chin. J. Anal. Chem.* **2008**, *36*, 1011–1016.

29. Trojanowicz, M. *Trend. Anal. Chem.* **2006**, *25*, 480–489.

30. Jo, S.; Jeong, H.; Bae, S. R.; Jeon, S. *Microchem. J.* **2008**, *88*, 1–6.

31. Wang, H. S.; Li, T. H.; Jia, W. L.; Xu, H. Y. *Biosens. Bioelectron.* **2006**, *22*, 664–669.

32. Dursun, Z.; Gelmez, B. *Electroanalysis* **2010**, *22*, 1106–1114.

33. Shahrokhian, S.; Zare-Mehrjardi, H. R. *Electroanal.* **2007**, *19*, 2234–2242.

34. Habibi, B.; Pournaghi-Azar, M. H. *Electrochim. Acta* **2010**, *55*, 5492–5498.

35. Yan, Q.; Zhao, F.; Liu, G.; Zeng, B. *Electroanal.* **2006**, *18*, 1075–1080.

36. Wu, Y.; Hu, S. *Colloid. Surf. B* **2005**, *41*, 299–304.

37. Zhang, M.; Gorski, W. *J. Am. Chem. Soc.* **2005**, *127*, 2058–2059.

38. Luque, G. L.; Ferrayra, N. F.; Rivas, G. A. *Talanta* **2007**, *71*, 1282–1287.

39. Dai, X.; Wildgoose, G. G.; Compton, R. G. *Analyst* **2006**, *131*, 1241–1247.

40. Guo, M.; Chen, J.; Li, J.; Tao, B.; Yao, S. *Anal. Chim. Acta* **2005**, *532*, 71–77.

41. Heng, L. Y.; Chou, A.; Yu, J.; Chen, Y.; Gooding, J. J. *Electrochem. Comm.* **2005**, *7*, 1457–1462.

42. Ye, Y.; Ju, H. *Biosens. Bioelectron.* **2005**, *21*, 735–741.

43. Xu, Y.; Ye, X.; Yang, L.; He, P.; Fang Y. *Electroanal.* **2006**, *18*, 1471–1478.

44. Goyal, R. N.; Kumar, A.; Mittal, A. *J. Chem. Soc. Perkin Trans.* **1991**, *2*, 1369–1375.

45. Da Silva, L. M.; De Faria, L. A.; Boodts, J. F. C. *Electrochim. Acta* **2003**, *48*, 699–709.

46. Miller, B.; Chen, A.; *Electrochim. Acta* **2005**, *50*, 2203–2212.